CORA Cork Open Research Archive
Cartlann Taighde Oscailte Chorcaí

Title	Broadband quantum dot micro-light-emitting diodes with parabolic sidewalls
Author(s)	Tanriseven, Selim; Maaskant, Pleun P.; Corbett, Brian M.
Publication date	2008
Original citation	Tanriseven, S., Maaskant, P. and Corbett, B. (2008) 'Broadband quantum dot micro-light-emitting diodes with parabolic sidewalls', Applied Physics Letters, 92(12), pp. 123501. doi: 10.1063/1.2898731
Type of publication	Article (peer-reviewed)
Link to publisher's version	http://aip.scitation.org/doi/abs/10.1063/1.2898731 http://dx.doi.org/10.1063/1.2898731 Access to the full text of the published version may require a subscription.
Rights	**© 2008 American Institute of Physics.This article may be downloaded for personal use only. Any other use requires prior permission of the author and AIP Publishing. The following article appeared in Tanriseven, S., Maaskant, P. and Corbett, B. (2008) 'Broadband quantum dot micro-light-emitting diodes with parabolic sidewalls', Applied Physics Letters, 92(12), pp. 123501 and may be found at http://aip.scitation.org/doi/abs/10.1063/1.2898731**
Item downloaded from	http://hdl.handle.net/10468/4372

UCC

University College Cork, Ireland
Coláiste na hOllscoile Corcaigh

Broadband quantum dot micro-light-emitting diodes with parabolic sidewalls

Selim Tanriseven, Pleun Maaskant, and Brian Corbett

Articles you may be interested in

Broadband quantum dot micro-light-emitting diodes with parabolic sidewalls

Selim Tanriseven,[a] Pleun Maaskant, and Brian Corbett

Tyndall National Institute, Lee Maltings, Prospect Row, Cork, Ireland

Arrays of long wavelength, self-organized InGaAs quantum dot micron sized light-emitting diodes (μ-LEDs) with parabolic sidewalls are introduced. The parabolic profiles of the μ-LEDs produced by resist reflow and controlled dry etching improve the extraction efficiency from the LEDs by redirection of the light into the escape cone by reflection from the sidewalls. A fourfold increase in the substrate emitted power density compared to a reference planar LED is measured. The reflected light is verified to be azimuthally polarized. The spectral width of the emission can be greater than 200 nm. © *2008 American Institute of Physics*. [DOI: 10.1063/1.2898731]

High-efficiency light-emitting diodes (LEDs) are desired for applications in short-haul data communications and as a light source in optical sensors and optical displays. However, the external quantum efficiency of conventional GaAs based LEDs is usually only a few percent compared to internal quantum yield, which can exceed 90%. This is due to the small ($\sim 16°$) escape cone θ_c for the light generated in the high refractive index ($n_s = 3.5$) semiconductor material, resulting in only 2% of the internally generated light escaping per planar surface. The remainder of the light suffers total internal reflection and absorption. A number of strategies have been employed to improve the extraction efficiency by using surface roughening, chip shaping, and nonresonant or resonant cavity effects.[1–5] In this letter, we introduce a way to improve light extraction by using arrays of micron sized LEDs (μ-LEDs) with parabolic sidewalls to direct the emission through the transparent substrate. The active region contains self-assembled In(Ga)As quantum dots (QDs) on a GaAs substrate. QDs are becoming an important active medium in lasers for telecommunications[6–8] due to their low transparency current, controllable chirp parameter, and low sensitivity to feedback. QDs also offer some significant advantages if they are used as the active medium in LEDs. The inhomogeneous broadening permits wide bandwidth emission used in edge emitting superluminescent LEDs,[9] while the short carrier diffusion length reduces the effect of surface recombination at exposed *p-n* junctions.[10] The GaAs substrate is transparent to the emission from the dots and processing techniques, such as selective oxidation, can be employed.

The principle behind the μ-LED approach can be understood by reference to Fig. 1, which shows an individual element of the proposed array. The sidewalls of the LED are shaped in the form of a parabola with the active region as the focus. The sidewalls are coated with a protective dielectric layer and the metal used in the *p*-type contact. All rays of light emitted from the focus and reflected off the parabolic surface will result in a parallel beam of light directed toward the surface and, thus, be within the escape cone. This necessitates either total internal reflection or high reflection from the metal coated sidewalls. The light emission from the structure can be partitioned into three regions. The first re-

gion is the conventional escape cone, which subtends a solid angle of $2\pi(1 - \cos \theta_c) = 2\pi(0.04 \text{ sr})$. The second region includes the rays from the critical angle to the base of the parabola, i.e., between θ_c and $\theta_b = \tan^{-1}(D/2h)$, where D is the diameter of the base and h is the depth from the active layer to the base of the parabola. For a typical structure with a base radius of 5 μm and a h of 2.5 μm, $\theta_b = 63.4°$ and the region subtends a solid angle of $2\pi(0.51 \text{ sr})$. In that region, light undergoes reflection from the planar substrate and is ultimately lost by absorption. The remainder is the third region and covers a solid angle of $2\pi(1.45 \text{ sr})$, and light emitted into that region will be partially or totally internally reflected from the sidewalls of the parabola toward the escape cone. For $h/D = 1$, almost half the light emitted into the lower hemisphere undergoes partial reflection from the parabola.

A larger h/D will increase that value. This analysis assumes isotropic emission from the focus of the parabola. To confine the emission close to the focus, selective oxidation of an AlGaAs layer is employed. Because of the high refractive index contrast between AlO$_x$ and GaAs, there will be strong waveguiding, with subsequent reflection at the sidewall.

The evolution of electric field intensity in a μ-LED is simulated by two-dimensional finite difference time domain (FDTD) method by using the freely available software package MEEP.[11] A still image of the simulated electric field of a typical μ-LED showing the redirection of light toward the substrate and the directional emission pattern is shown in Fig. 2.

Arrays of μ-LEDs were fabricated on an epitaxial wafer grown on a *n*-doped GaAs substrate from NL Nanosemicon-
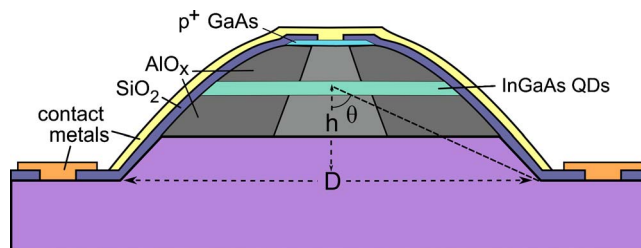

FIG. 1. (Color online) Schematic diagram of an individual μ-LED. Current is directed toward the focus of the parabola by using selective oxidation, while the surface of the parabola is coated with SiO$_2$ to prevent shorting.

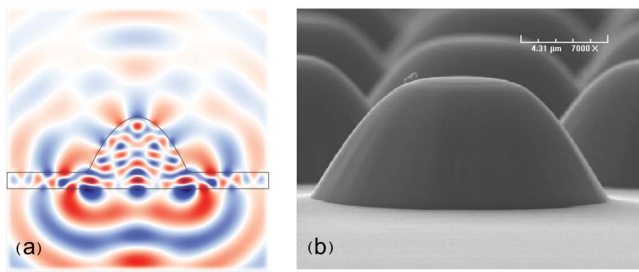[a]Electronic mail: selim.tanriseven@tyndall.ie.

FIG. 2. (Color online) (a) Two-dimensional FDTD simulated electric field intensity distribution from a μ-LED. The parabola is simulated as the slice of a cone with a plane that is parallel to a line on the cone through its vertex. (b) SEM picture of a μ-LED mesa after dry etch and resist removal showing the parabolic-shaped sidewalls.

ductor GmbH by using molecular beam epitaxy. The layer structure contains a separate confinement heterostructure with 900 nm thick, n- and p-doped $Al_{0.9}Ga_{0.1}As$ outer claddings and a 115 nm thick $Al_{0.35}Ga_{0.65}As$ layers linearly graded down to GaAs in the last 15 nm. The active layer consists of five stacks of self-organized InAs QDs inside $In_{0.15}Ga_{0.85}As$ quantum wells with 33 nm GaAs spacer layers between each dot layer. The structure is completed with a 200 nm thick heavily p-doped GaAs cap layer. The peak photoluminescence wavelength is located at around 1265 nm.

The fabrication process of the μ-LEDs begins with defining an array of photoresist cylinders of 17 μm diameter by standard photolithography techniques. After development, the photoresist is reflowed at 140 °C for 2 h. The base diameter of the resist remains constant during the reflow, provided that resist wetting of the substrate is avoided. This is verified by scanning electron micrograph (SEM) images. For larger resist diameters, the center of the resist collapses because the surface tension is not sufficient to maintain a spherical surface. Subsequently, the resist structure is transferred into the epilayers by an inductively coupled plasma etch process with BCl_3 chemistry, resulting in 5 μm high semiconductor mesa structures. The selectivity of the etch process between the resist and the material was optimized to obtain the desired curvature of the sidewalls (Fig. 2). After removing the photoresist mask, the samples are placed in a furnace at 405 °C in a water vapor ambient for an hour to selectively oxidize the $Al_{0.9}Ga_{0.1}As$ layers to a penetration depth of 2 μm. Following sidewall passivation with SiO_2 and opening of 5 μm diameter windows in the passivation layer for p contacts, Ti/Pt/Au is deposited by electron beam evaporation. n-contact pads are defined on the epitaxial side with a Au/Ge/Ni/Au alloy. The GaAs substrate was polished, but no coating was applied.

The light-current (LI) characteristics of a 16×16 μ-LED array and a reference (planar) 600 μm diameter contact are shown in Fig. 3. The emission is collected through the substrate with a 7 mm^2 disk-shaped Ge detector located at a distance of 9 mm, resulting in a collecting numerical aperture (NA) of 0.16. Since the emitting dimensions are not the same for each device, the power densities (ratio of the power output to active area) are compared. The total active area of the μ-LED array is estimated by calculating the active area of each device by using the diameter measured from the SEM images, multiplied by the number of emitting devices in the array. The μ-LED efficiency into the NA of 0.16
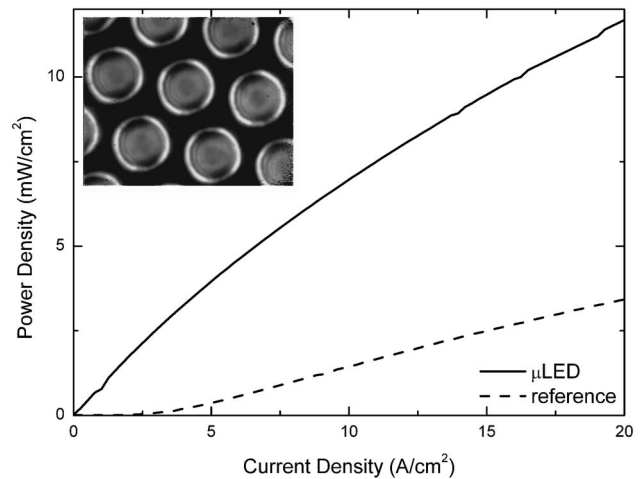

FIG. 3. Light-current characteristics of μ-LEDs compared to that of a broad area reference LED. A fourfold increase in forward emitted power density at 20 A/cm^2 is observed. Near-field image is in the inset. Reflection from the sidewalls is clearly visible as bright rings.

is about four times higher than that of the reference LED at an operating current density of 20 A/cm^2.

At low currents, the power from the μ-LED into the limited NA is greater than the planar device, despite the fact that about 60% of the active area is removed to form a close packed hexagonal arrangement of μ-LEDs with a 5 μm deep etch. While the total power into all angles can be less with the μ-LED, the μ-LED yields enhanced brightness (power/steradian) and a higher extraction efficiency. At higher current densities, the LI characteristic of the μ-LEDs becomes sublinear due to band-filling effects (see Fig. 4) in the limited number of QD layers used here.

Near-field images of the μ-LEDs are captured by imaging the emission from the substrate onto a charge coupled device camera. A typical image is shown in the inset of Fig. 3. Light reflected off the sidewalls and redirected into escape cone is visible as bright rings around each device. The rings are expected to be azimuthally polarized if they result from reflection of the TE polarized QD emission off the sidewalls. This is verified by rotating a linear polarizer between the lens
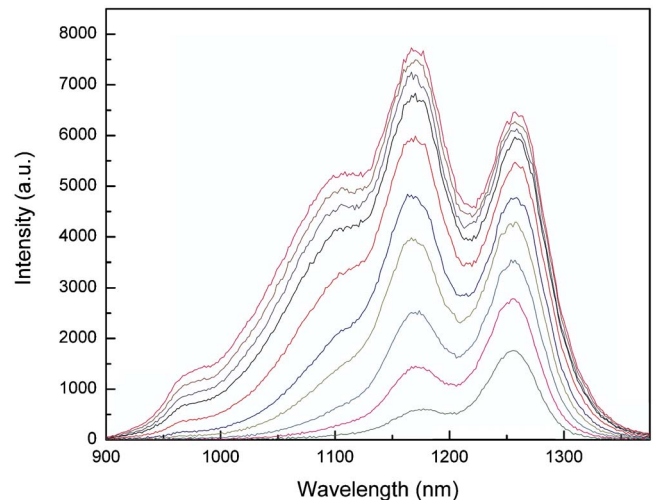

FIG. 4. (Color online) Electroluminescence spectra from a μ-LED array for increasing currents from 0.1 to 5 mA, from bottom to top. 5 mA, current injection corresponds to a current density of 350 A/cm^2 wherein the spectral full width at half maximum is 225 nm.

and the camera. This can also be seen in the near-field image in which the dark parts of the ring along a vertical line are due to the azimuthal polarization along with polarization by reflection from a mirror in the optical path of the near-field setup. The light extraction efficiency enhancement can be estimated by taking the ratio of the integrated intensity of a device over all of its area to the integrated intensity in the center of the device excluding the rings. This ratio is about 4, verifying the extraction efficiency enhancement figure obtained from the *LI* plot. Further improvement in efficiency can be expected with a more reflective contact metallization and deeper etched mesas.

The electroluminescence emission spectra of a μ-LED array at various injection current densities are presented in Fig. 4. At low injection current, the emission peak is at around 1265 nm with the ground state (GS) of the QD dominating the spectrum. With increasing injection current, the carriers begin to fill the excited states (ESs) and the states of the InGaAs well before saturating the GS and ESs, resulting in a significant broadening of the emission spectrum. At 5 mA current injection, which corresponds to a current density of 350 A/cm^2, the device has a broad emission spectrum of 225 nm. The broad emission and directionality of the μ-LEDs make them useful in applications such as optical coherence tomography.

In conclusion, we have presented a structural design for improving the extraction efficiency from substrate emitting LEDs. A fourfold increase in forward emitted power density compared to that of unpatterned reference LEDs is measured. Near-field imaging verifies the contribution of reflected light to the emission. Broad emission spectra are realized from QD active media. Increasing the aspect ratio of the μ-LEDs will result in increased extraction efficiency while simultaneously reducing the divergence of the emission. Scaling the dimensions of a μ-LED to one containing a single QD may result in a single photon source that can be coupled to a fiber effectively.

[1] I. Schnitzer, E. Yablonovitch, C. Caneau, T. J. Gmitter, and A. Scherer, Appl. Phys. Lett. **63**, 2174 (1993).

[2] M. R. Krames, M. Ochiai-Holcomb, G. E. Hofler, C. Carter-Coman, E. I. Chen, I.-H. Tan, P. Grillot, N. F. Gardner, H. C. Chui, J.-W. Huang, S. A. Stockman, F. A. Kish, M. G. Craford, T. S. Tan, C. P. Kocot, M. Hueschen, J. Posselt, B. Loh, G. Sasser, and D. Collins, Appl. Phys. Lett. **75**, 2365 (1999).

[3] R. Windisch, B. Dutta, M. Kuijk, A. Knobloch, S. Meinlschmidt, S. Schoberth, P. Kiesel, G. Borghs, G. H. Döhler, and P. Heremans, IEEE Trans. Electron Devices **47**, 1492 (2000).

[4] D. Delbeke, R. Bockstaele, P. Bienstman, R. Baets, and H. Benisty, IEEE J. Sel. Top. Quantum Electron. **8**, 189 (2002).

[5] K. Streubel, N. Linder, R. Wirth, and A. Jaeger, IEEE J. Sel. Top. Quantum Electron. **8**, 321 (2002).

[6] G. T. Liu, A. Stintz, H. Li, K. J. Malloy, and L. F. Lester, Electron. Lett. **35**, 1163 (1999).

[7] F. Schäfer, J. P. Reithmaier, and A. Forchel, Appl. Phys. Lett. **74**, 2915 (1999).

[8] A. J. Shields, Nat. Photonics **1**, 215 (2007).

[9] M. Rossetti, L. Li, A. Markus, A. Fiore, L. Occhi, C. Vélez, S. Mikhrin, I. Krestnikov, and A. Kovsh, IEEE J. Quantum Electron. **43**, 676 (2007).

[10] S. A. Moore, L. O'Faolain, M. A. Cataluna, M. B. Flynn, M. V. Kotlyar, and T. F. Krauss, IEEE Photonics Technol. Lett. **18**, 1861 (2006).

[11] A. Farjadpour, D. Roundy, A. Rodriguez, M. Ibanescu, P. Bermel, J. D. Joannopoulos, S. G. Johnson, and G. Burr, Opt. Lett. **31**, 2972 (2006).